Published in final edited form as:
Mol Pharm. 2013 September 3; 10(9): 3417–3424. doi:10.1021/mp400248f.

Evaluation of New Tc-99m-Labeled Arg-X-Asp-Conjugated Alpha-Melanocyte Stimulating Hormone Peptides for Melanoma Imaging

Adam M. Flook[†], **Jianquan Yang**[†], and **Yubin Miao**[†,‡,§,*]

[†]College of Pharmacy, University of New Mexico, Albuquerque, NM 87131, USA

[‡]Cancer Research and Treatment Center, University of New Mexico, Albuquerque, NM 87131, USA

[§]Department of Dermatology, University of New Mexico, Albuquerque, NM 87131, USA

Abstract

The purpose of this study was to examine the melanoma targeting and imaging properties of two new ^{99m}Tc-labeled Arg-X-Asp-conjugated alpha-melanocyte stimulating hormone (α-MSH) peptides. RTD-Lys-(Arg^{11})CCMSH {c[Asp-Arg-Thr-Asp-DTyr]-Lys-Cys-Cys-Glu-His-DPhe-Arg-Trp-Cys-Arg-Pro-Val-NH_2} and RVD-Lys-(Arg^{11})CCMSH peptides were synthesized and their melanocortin-1 (MC1) receptor binding affinities were determined in B16/F1 melanoma cells. The biodistribution and melanoma imaging properties of ^{99m}Tc-RTD-Lys-(Arg^{11})CCMSH and ^{99m}Tc-RVD-Lys-(Arg^{11})CCMSH were determined in B16/F1 melanoma-bearing C57 mice. The IC_{50} values of RTD-Lys-(Arg^{11})CCMSH and RVD-Lys-(Arg^{11})CCMSH were 0.7 ± 0.07 and 1.0 ± 0.3 nM in B16/F1 melanoma cells. Both ^{99m}Tc-RTD-Lys-(Arg^{11})CCMSH and ^{99m}Tc-RVD-Lys-(Arg^{11})CCMSH displayed high melanoma uptake. ^{99m}Tc-RTD-Lys-(Arg^{11})CCMSH exhibited the peak tumor uptake of 18.77 ± 5.13% ID/g at 2 h post-injection, whereas ^{99m}Tc-RVD-Lys-(Arg^{11})CCMSH reached the peak tumor uptake of 19.63 ± 4.68% ID/g at 4 h post-injection. Both ^{99m}Tc-RTD-Lys-(Arg^{11})CCMSH and ^{99m}Tc-RVD-Lys-(Arg^{11})CCMSH showed low accumulation in normal organs (<1.7% ID/g) except for the kidneys at 2 h post-injection. The renal uptake of ^{99m}Tc-RTD-Lys-(Arg^{11})CCMSH and ^{99m}Tc-RVD-Lys-(Arg^{11})CCMSH was 135.14 ± 23.62 and 94.01 ± 18.31% ID/g at 2 h post-injection, respectively. The melanoma lesions were clearly visualized by SPECT/CT using either ^{99m}Tc-RTD-Lys-(Arg^{11})CCMSH or ^{99m}Tc-RVD-Lys-(Arg^{11})CCMSH as an imaging probe at 2 h post-injection. Overall, the introduction of Thr or Val residue retained high melanoma uptake of ^{99m}Tc-RTD-Lys-(Arg^{11})CCMSH and ^{99m}Tc-RVD-Lys-(Arg^{11})CCMSH. However, high renal uptake of ^{99m}Tc-RTD-Lys-(Arg^{11})CCMSH and ^{99m}Tc-RVD-Lys-(Arg^{11})CCMSH need to be reduced to facilitate their future applications.

Keywords

Receptor-targeting; alpha-melanocyte stimulating hormone peptide; melanoma imaging

Corresponding Author: Yubin Miao, 2502 Marble NE, MSC09 5360, College of Pharmacy, University of New Mexico, Albuquerque, NM 87131-0001. Phone: (505) 925-4437; Fax: (505) 272-6749; ymiao@salud.unm.edu.

INTRODUCTION

Malignant melanoma is the most lethal form of skin cancer with an increasing incidence.[1] Melanoma leads to greater than 75% of deaths from skin cancer although it only accounts for less than 5% of skin cancer cases. There is no curative treatment available for metastatic melanoma. Both melanocortin-1 (MC1) and $\alpha_v\beta_3$ integrin receptors have been utilized as targets for developing melanoma imaging probes.[2–22] The radiolabeled α-melanocyte stimulating hormone (α-MSH) peptides were used to target the MC1 receptors,[2–14] whereas the radiolabeled Arg-Gly-Asp (RGD) peptides were reported to target the $\alpha_v\beta_3$ integrin receptors.[15–22] In our previous report, we developed a novel Arg-Gly-Asp (RGD)-conjugated α-MSH hybrid peptide {RGD-Lys-(Arg^{11})CCMSH} to target both MC1 and $\alpha_v\beta_3$ integrin receptors for M21 human melanoma imaging.[23] The dual receptor-targeting ^{99m}Tc-RGD-Lys-(Arg^{11})CCMSH exhibited significantly higher melanoma uptake than single receptor-targeting ^{99m}Tc-RAD-Lys-Arg^{11})CCMSH or ^{99m}Tc-RGD-Lys-(Arg^{11})CCMSHscramble in M21 human melanoma-xenografted nude mice. Interestingly, the switch from RGD to Arg-Ala-Asp (RAD) in the hybrid peptide dramatically improved the MC1 receptor binding affinity of RAD-Lys-(Arg^{11})CCMSH as compared to RGD-Lys-(Arg^{11})CCMSH (0.3 vs. 2.0 nM) in M21 melanoma cells.[23] The stronger MC1 receptor binding resulted in enhanced melanoma uptake of ^{99m}Tc-RAD-Lys-(Arg^{11})CCMSH as compared with ^{99m}Tc-RGD-Lys-(Arg^{11})CCMSH (19.91 ± 4.02 vs. 14.83 ± 2.93% ID/g at 2 h post-injection) in B16/F1 melanoma-bearing C57 mice.[24]

The minor structural difference between ^{99m}Tc-RAD-Lys-(Arg^{11})CCMSH and ^{99m}Tc-RGD-Lys-(Arg^{11})CCMSH is Ala and Gly. The Ala has one more methyl group as compared with the Gly. The biodistribution results indicated that the existence of methyl group in Ala enhanced the melanoma uptake of ^{99m}Tc-RAD-Lys-(Arg^{11})CCMSH.[24] Therefore, we were interested in whether the substitution of Gly with other amino acids could affect the melanoma targeting and pharmacokinetic properties of ^{99m}Tc-labeled peptides. In this study, we replaced the Gly with Thr and Val to generate RTD-Lys-(Arg^{11})CCMSH and RVD-Lys-(Arg^{11})CCMSH peptides. The MC1 receptor binding affinities of RTD-Lys-(Arg^{11})CCMSH and RVD-Lys-(Arg^{11})CCMSH were examined in B16/F1 melanoma cells. Thereafter, we determined the biodistribution and imaging properties of ^{99m}Tc-RTD-Lys-(Arg^{11})CCMSH and ^{99m}Tc-RVD-Lys-(Arg^{11})CCMSH in B16/F1 melanoma-bearing C57 mice.

EXPERIMENTAL SECTION

Chemicals and Reagents

Amino acids and resin were purchased from Advanced ChemTech Inc. (Louisville, KY) and Novabiochem (San Diego, CA). ^{125}I-Tyr^2-[Nle^4, DPhe^7]-α-MSH {^{125}I-(Tyr^2)-NDP-MSH} was obtained from PerkinElmer, Inc. (Waltham, MA) for receptor binding assay. $^{99m}TcO_4^-$ was purchased from Cardinal Health (Albuquerque, NM). *L*-lysine was purchased from Sigma-Aldrich (St. Louis, MO). All other chemicals used in this study were purchased from Thermo Fischer Scientific (Waltham, MA) and used without further purification. B16/F1 murine melanoma cells were obtained from American Type Culture Collection (Manassas, VA).

Peptide Synthesis and *In Vitro* Competitive Binding Assay

The RTD-Lys-(Arg^{11})CCMSH and RVD-Lys-(Arg^{11})CCMSH peptides were synthesized according to our previously published procedure[25] with slight modification on Sieber amide resin by an Advanced ChemTech multiple-peptide synthesizer (Louisville, KY). Briefly, 70 μmol of Sieber amide resin and 210 μmol of Fmoc-protected amino acids were used for the synthesis. Fmoc-Lys(Boc) was used to generate a Lys linker in the hybrid peptide. The

RTD-Lys-(Arg^{11})CCMSH and RVD-Lys-(Arg^{11})CCMSH were purified by reverse phase-high performance liquid chromatography (RP-HPLC) and characterized by liquid chromatography-mass spectroscopy (LC-MS).

The IC_{50} values RTD-Lys-(Arg^{11})CCMSH and RVD-Lys-(Arg^{11})CCMSH for the MC1 receptor were determined in B16/F1 melanoma cells. The receptor binding assay was replicated in triplicate for each peptide. The B16/F1 cells were seeded into a 24-well cell culture plate at a density of 2.5×10^5 cells/well and incubated at 37° C overnight. After being washed with binding medium {modified Eagle's medium with 25 mM N-(2-hydroxyethyl)-piperazine-N′-(2-ethanesulfonic acid) (HEPES), pH 7.4, 0.2% bovine serum albumin (BSA), 0.3 mM 1,10-phenathroline}, the cells were incubated at 25 °C for 2 h with approximately 30,000 counts per minute (cpm) of ^{125}I-(Tyr^2)-NDP-MSH in the presence of increasing concentrations (10^{-13} M to 10^{-6} M) of RTD-Lys-(Arg^{11})CCMSH or RVD-Lys-(Arg^{11})CCMSH in 0.3 mL of binding medium. The reaction medium was aspirated after the incubation. The cells were rinsed twice with 0.5 mL of ice-cold pH 7.4, 0.2% BSA/0.01 M phosphate buffered saline (PBS) to remove any unbound radioactivity and lysed in 0.5 mL of 1 M NaOH for 5 min. The activities associated with the cells were measured in a Wallac 1480 automated gamma counter (PerkinElmer, NJ). The IC_{50} value for each peptide was calculated using Prism software (GraphPad Software, La Jolla, CA).

Peptide Radiolabeling

RTD-Lys-(Arg^{11})CCMSH and RVD-Lys-(Arg^{11})CCMSH peptides were labeled with ^{99m}Tc via a direct reduction reaction with $SnCl_2$. Briefly, 10 μL of 1 mg/mL $SnCl_2$ in 0.1 M HCl, 40 μL of 0.5 M NH_4OAc (pH 5.2), 100 μL of 0.2 M Na_2tartate (pH 9.2), 100 μL of fresh $^{99m}TcO_4^-$ solution (37–74 MBq), and 10 μL of 1 mg/mL RTD-Lys-(Arg^{11})CCMSH or RVD-Lys-(Arg^{11})CCMSH peptide in aqueous solution were added into a reaction vial and incubated at 25 °C for 20 min to form ^{99m}Tc-labeled peptide. Each ^{99m}Tc-peptide was purified to a single species by Waters RP-HPLC (Milford, MA) on a Grace Vydac C-18 reverse phase analytic column (Deerfield, IL) using a 20-min gradient of 16–26% acetonitrile in 20 mM HCl aqueous solution at a flow rate of 1 mL/min. Each purified peptide was purged with N_2 gas for 20 mins to remove the acetonitrile. The pH of final peptide solution was adjusted to 7.4 with 0.1 N NaOH and sterile normal saline for stability, biodistribution and imaging studies. The serum stability of ^{99m}Tc-RTD-Lys-(Arg^{11})CCMSH and ^{99m}Tc-RVD-Lys-(Arg^{11})CCMSH was determined by incubation in mouse serum at 37 °C for 24 h and monitored for degradation by RP-HPLC. Briefly, 100 μL of HPLC-purified peptide solution (∼7.4 MBq) was added into 100 μL of mouse serum (Sigma-Aldrich Corp, St. Louis, MO) and incubated at 37°C for 24 h. After the incubation, 200 μL of a mixture of ethanol and acetonitrile (V:V = 1:1) was added to precipitate the serum proteins. The resulting mixture was centrifuged at 16,000 g for 5 min to collect the supernatant. The supernatant was purged with N_2 gas for 30 min to remove the ethanol and acetonitrile. The resulting sample was mixed with 500 μL of water and injected into RP-HPLC for analysis using the gradient described above.

Cellular Internalization and Efflux

Cellular internalization and efflux of ^{99m}Tc-RTD-Lys-(Arg^{11})CCMSH and ^{99m}Tc-RVD-Lys-(Arg^{11})CCMSH were evaluated in B16/F1 melanoma cells. The B16/F1 cells were seeded into a 24-well cell culture plate at a density of 2.5×10^5 cells/well and incubated at 37° C overnight. After being washed twice with binding medium [modified Eagle's medium with 25 mM *N*-(2-hydroxyethyl)-piperazine-*N*'-(2-ethanesulfonic acid), pH 7.4, 0.2% bovine serum albumin (BSA), 0.3 mM 1,10-phenathroline], the B16/F1 cells were incubated at 25°C for 20, 40, 60, 90 and 120 min (n=3) in the presence of approximate 200,000 counts per minute (cpm) of HPLC-purified of ^{99m}Tc-RTD-Lys-(Arg^{11})CCMSH or ^{99m}Tc-RVD-

Lys-(Arg^{11})CCMSH. After incubation, the reaction medium was aspirated and the cells were rinsed with 2 × 0.5 mL of ice-cold pH 7.4, 0.2% BSA / 0.01 M PBS. Cellular internalization was assessed by washing the cells with acidic buffer [40 mM sodium acetate (pH 4.5) containing 0.9% NaCl and 0.2% BSA] to remove the membrane-bound radioactivity. The remaining internalized radioactivity was obtained by lysing the cells with 0.5 mL of 1 N NaOH for 5 min. Membrane-bound and internalized activities were counted in a gamma counter. Cellular efflux was determined by incubating the B16/F1 cells with ^{99m}Tc-RTD-Lys-(Arg^{11})CCMSH or ^{99m}Tc-RVD-Lys-(Arg^{11})CCMSH for 2 h at 25°C, removing non-specific-bound activity with 2 × 0.5 mL of ice-cold PBS rinse, and monitoring radioactivity released into cell culture medium. At time points of 20, 40, 60, 90 and 120 min, the radioactivities on the cell surface and inside the cells were separately collected and counted in a gamma counter.

Biodistribution Studies

All the animal studies were conducted in compliance with Institutional Animal Care and Use Committee approval. The biodistribution properties of ^{99m}Tc-RTD-Lys-(Arg^{11})CCMSH and ^{99m}Tc-RVD-Lys-(Arg^{11})CCMSH were determined in B16/F1 melanoma-bearing C57 female mice (Harlan, Indianapolis, IN). Each C57 mouse was subcutaneously inoculated on the right flank with 1×10^6 B16/F1 cells. The weight of tumors reached approximately 0.2 g 10 days post cell inoculation. Each melanoma-bearing mouse was injected with 0.037 MBq of ^{99m}Tc-RTD-Lys-(Arg^{11})CCMSH and ^{99m}Tc-RVD-Lys-(Arg^{11})CCMSH via the tail vein. Groups of 4 mice were sacrificed at 0.5, 2, 4 and 24 h post-injection, and tumors and organs of interest were harvested, weighed and counted. Blood values were taken as 6.5% of the body weight. The specificity of tumor uptake was determined by co-injecting ^{99m}Tc-RTD-Lys-(Arg^{11})CCMSH or ^{99m}Tc-RVD-Lys-(Arg^{11})CCMSH with 10 μg (6.1 nmol) of unlabeled NDP-MSH at 2 h post-injection.

L-lysine co-injection is effective in decreasing the renal uptake of radiolabeled α-MSH peptides. To determine the effect of *L*-lysine co-injection on the renal uptake of ^{99m}Tc-RTD-Lys-(Arg^{11})CCMSH and ^{99m}Tc-RVD-Lys-(Arg^{11})CCMSH, a group of 4 mice were injected with a mixture of 0.037 MBq of ^{99m}Tc-RTD-Lys-(Arg^{11})CCMSH or ^{99m}Tc-RVD-Lys-(Arg^{11})CCMSH and 15 mg of *L*-lysine. The mice were sacrificed at 2 h post-injection, and tumors and organs of interest were harvested, weighed and counted in a gamma counter.

Melanoma Imaging with ^{99m}Tc-RTD-Lys-(Arg^{11})CCMSH and ^{99m}Tc-RVD-Lys-(Arg^{11})CCMSH

To determine the melanoma imaging properties, approximately 7.4 MBq of ^{99m}Tc-RTD-Lys-(Arg^{11})CCMSH or ^{99m}Tc-RVD-Lys-(Arg^{11})CCMSH was injected into two B16/F1 melanoma-bearing C57 mice via the tail vein, respectively. The mice were euthanized for small animal SPECT/CT (Nano-SPECT/CT®, Bioscan, Washington DC) imaging 2 h post-injection. The 9-min CT imaging was immediately followed by the SPECT imaging of whole-body. The SPECT scans of 24 projections were acquired. Reconstructed data from SPECT and CT were visualized and co-registered using InVivoScope (Bioscan, Washington DC).

Urinary Metabolites of ^{99m}Tc-RTD-Lys-(Arg^{11})CCMSH and ^{99m}Tc-RVD-Lys-(Arg^{11})CCMSH

Approximately 3.7 MBq of ^{99m}Tc-RTD-Lys-(Arg^{11})CCMSH or ^{99m}Tc-RVD-Lys-(Arg^{11})CCMSH was injected into two B16/F1 melanoma-bearing C57 mice via the tail vein to determine the urinary metabolites. The mice were euthanized to collect urine at 2 h post-injection. The collected urine samples were centrifuged at 16,000 g for 5 min before the HPLC analysis. Thereafter, aliquots of the urine were injected into the HPLC. A 20-minute gradient of 16–26% acetonitrile / 20 mM HCl with a flow rate of 1 mL/min was used for urine analysis.

Statistical Analysis

Statistical analysis was performed using the Student's t-test for unpaired data to determine the significance of differences in tumor and kidney uptake with/without peptide blockade or with/without *L*-lysine co-injection in biodistribution studies described above. Differences at the 95% confidence level ($p<0.05$) were considered significant.

RESULTS

The schematic structures of RTD-Lys-(Arg^{11})CCMSH and RVD-Lys-(Arg^{11})CCMSH are presented in Figure 1. RTD-Lys-(Arg^{11})CCMSH and RVD-Lys-(Arg^{11})CCMSH were synthesized and purified by RP-HPLC. The overall synthetic yields were 30% for RTD-Lys-(Arg^{11})CCMSH and RVD-Lys-(Arg^{11})CCMSH. The chemical purities of RTD-Lys-(Arg^{11})CCMSH and RVD-Lys-(Arg^{11})CCMSH were greater than 95% after the HPLC purification. The peptide identities were confirmed by electrospray mass spectrometry. The measured molecular weights for RTD-Lys-(Arg^{11})CCMSH and RVD-Lys-(Arg^{11})CCMSH were 2194 and 2192. The competitive binding curves of the peptides are shown in Figure 2. The IC_{50} values of RTD-Lys-(Arg^{11})CCMSH and RVD-Lys-(Arg^{11})CCMSH were 0.7 ± 0.07 and 1.0 ± 0.3 nM in B16/F1 melanoma cells.

RTD-Lys-(Arg^{11})CCMSH and RVD-Lys-(Arg^{11})CCMSH were readily radiolabeled with ^{99m}Tc with greater than 95% radiolabeling yields. The ^{99m}Tc-RTD-Lys-(Arg^{11})CCMSH and ^{99m}Tc-RVD-Lys-(Arg^{11})CCMSH peptides were purified and separated from their excess non-labeled peptides by RP-HPLC. The retention times of ^{99m}Tc-RTD-Lys-(Arg^{11})CCMSH and ^{99m}Tc-RVD-Lys-(Arg^{11})CCMSH were 12.7 and 14.6 min. ^{99m}Tc-RTD-Lys-(Arg^{11})CCMSH and ^{99m}Tc-RVD-Lys-(Arg^{11})CCMSH were stable in mouse serum at 37°C for 24 h (Figure 3). Cellular internalization and efflux properties of ^{99m}Tc-RTD-Lys-(Arg^{11})CCMSH and ^{99m}Tc-RVD-Lys-(Arg^{11})CCMSH were examined in B16/F1 cells. Figure 4 illustrates the internalization and efflux properties of ^{99m}Tc-RTD-Lys-(Arg^{11})CCMSH and ^{99m}Tc-RVD-Lys-(Arg^{11})CCMSH. ^{99m}Tc-RTD-Lys-(Arg^{11})CCMSH and ^{99m}Tc-RVD-Lys-(Arg^{11})CCMSH exhibited rapid cellular internalization and prolonged cellular retention. Approximately 71% of ^{99m}Tc-RTD-Lys-(Arg^{11})CCMSH and 72% of ^{99m}Tc-RVD-Lys-(Arg^{11})CCMSH activities were internalized in the cells after 20 min of incubation. Cellular efflux results indicated that 75% of ^{99m}Tc-RTD-Lys-(Arg^{11})CCMSH and 70% of ^{99m}Tc-RVD-Lys-(Arg^{11})CCMSH activities remained inside the cells at 2 h of incubation in the culture medium.

The melanoma targeting and pharmacokinetic properties of ^{99m}Tc-RTD-Lys-(Arg^{11})CCMSH and ^{99m}Tc-RVD-Lys-(Arg^{11})CCMSH are shown in Tables 1 and 2. Both ^{99m}Tc-RTD-Lys-(Arg^{11})CCMSH and ^{99m}Tc-RVD-Lys-(Arg^{11})CCMSH exhibited rapid and high tumor uptake in B16/F1 melanoma-bearing C57 mice. ^{99m}Tc-RTD-Lys-(Arg^{11})CCMSH exhibited the peak tumor uptake of 18.77 ± 5.13% ID/g at 2 h post-injection, whereas ^{99m}Tc-RVD-Lys-(Arg^{11})CCMSH reached the peak tumor uptake of 19.63 ± 4.68% ID/g at 4 h post-injection. The tumor uptake values gradually decreased to 5.84 ± 0.50 and 8.81 ± 2.13% ID/g by 24 h post-injection. The tumor blocking studies (Tables 1–2) demonstrated that co-injection of 10 μg (6.1 nM) of non-radiolabeled NDP-MSH with ^{99m}Tc-RTD-Lys-(Arg^{11})CCMSH or ^{99m}Tc-RVD-Lys-(Arg^{11})CCMSH decreased their tumor uptake values to 2.85 ± 1.43 and 1.51 ± 0.6% ID/g at 2 h post-injection, demonstrating that the tumor uptake was MC1 receptor-mediated.

Renal uptake values of ^{99m}Tc-RTD-Lys-(Arg^{11})CCMSH and ^{99m}Tc-RVD-Lys-(Arg^{11})CCMSH were 135.14 ± 23.62 and 94.01 ± 18.31% ID/g at 2 h post injection, respectively. The renal uptake values of ^{99m}Tc-RTD-Lys-(Arg^{11})CCMSH and ^{99m}Tc-RVD-Lys-(Arg^{11})CCMSH decreased to 46.84 ± 14.83 and 44.34 ± 12.11% ID/g at 24 h post-

injection. The effect of *L*-lysine co-injection on renal uptake is presented in Figure 5. Co-injection of 15 mg *L*-lysine significantly ($p<0.05$) decreased the renal uptake values of ^{99m}Tc-RTD-Lys-(Arg^{11})CCMSH and ^{99m}Tc-RVD-Lys-(Arg^{11})CCMSH to 60.66 ± 12.09 and 55.74 ± 9.14% ID/g at 2 h post-injection, respectively. The *L*-lysine co-injection didn't affect the tumor uptake of ^{99m}Tc-RTD-Lys-(Arg^{11})CCMSH and ^{99m}Tc-RVD-Lys-(Arg^{11})CCMSH ($p>0.05$) at 2 h post-injection. Whole-body clearance of ^{99m}Tc-RTD-Lys-(Arg^{11})CCMSH and ^{99m}Tc-RVD-Lys-(Arg^{11})CCMSH was rapid, with approximately 55% and 59% of the injected radioactivity clearance through the urinary system by 2 h post-injection (Tables 1–2). At 24 h post-injection, 82% of ^{99m}Tc-RTD-Lys-(Arg^{11})CCMSH and 77% of ^{99m}Tc-RVD-Lys-(Arg^{11})CCMSH activity cleared out the body. Normal organ uptakes of ^{99m}Tc-RTD-Lys-(Arg^{11})CCMSH and ^{99m}Tc-RVD-Lys-(Arg^{11})CCMSH was minimal (<2.1% ID/g) except for the kidneys after 2 h post-injection (Tables 1–2).

Whole-body SPECT/CT images are presented in Figure 6. Flank B16/F1 melanoma lesions were clearly visualized by SPECT using ^{99m}Tc-RTD-Lys-(Arg^{11})CCMSH and ^{99m}Tc-RVD-Lys-(Arg^{11})CCMSH) peptides as imaging probes. The SPECT image of tumor accurately matched its anatomical location obtained in the CT image. The SPECT image showed high contrast of tumor to normal organ except for kidneys, which was consistent with the biodistribution results. The urinary metabolites of ^{99m}Tc-RTD-Lys-(Arg^{11})CCMSH and ^{99m}Tc-RVD-Lys-(Arg^{11})CCMSH at 2 h post-injection are shown in Figure 7. Approximately 70% of ^{99m}Tc-RTD-Lys-(Arg^{11})CCMSH or ^{99m}Tc-RVD-Lys-(Arg^{11})CCMSH remained intact in the urine at 2 h post-injection, while 30% of the ^{99m}Tc-RTD-Lys-(Arg^{11})CCMSH or ^{99m}Tc-RVD-Lys-(Arg^{11})CCMSH was transformed to a more hydrophobic compound.

DISCUSSION

We have been interested in developing MC1 receptor-targeting α-MSH peptides for melanoma imaging.[11–14,23–25] Recently, we have found that the substitution of RGD with RAD resulted in nearly a 10-fold increase in MC1 receptor binding affinity for RAD-Lys-(Arg^{11})CCMSH as compared to RGD-Lys-(Arg^{11})CCMSH in B16/F1 melanoma cells.[24] Furthermore, ^{99m}Tc-RAD-Lys-(Arg^{11})CCMSH displayed higher melanoma uptake than ^{99m}Tc-RGD-Lys-(Arg^{11})CCMSH (19.91 ± 4.02 vs. 14.83 ± 2.93% ID/g at 2 h post-injection) in B16/F1 melanoma-bearing C57 mice.[24] Because the only structural difference between ^{99m}Tc-RAD-Lys-(Arg^{11})CCMSH and ^{99m}Tc-RGD-Lys-(Arg^{11})CCMSH was the extra methyl group in Ala as compared to Gly, the enhanced melanoma uptake of ^{99m}Tc-RAD-Lys-(Arg^{11})CCMSH suggested that the methyl group in Ala dramatically affected the MC1 receptor binding motif (His-DPhe-Trp-Arg) in the (Arg^{11})CCMSH moiety. Thus, we were interested in whether and how the replacement of Gly with other amino acids could affect the melanoma targeting and pharmacokinetic properties of ^{99m}Tc-labeled RXD-Lys-(Arg^{11})CCMSH peptides. Specifically, we substituted the Gly with Thr and Val to examine the effects of -CH(CH$_3$)OH and -CH(CH$_3$)$_2$ groups on the biodistribution properties of ^{99m}Tc-labeled RTD-Lys-(Arg^{11})CCMSH and RVD-Lys-(Arg^{11})CCMSH peptides in this study.

The substitution of Gly with Thr and Val retained low nanomolar MC1 receptor binding affinities of the peptides in B16/F1 melanoma cells. RTD-Lys-(Arg^{11})CCMSH and RVD-Lys-(Arg^{11})CCMSH exhibited stronger MC1 receptor binding affinities than RGD-Lys-(Arg^{11})CCMSH and weaker MC1 receptor binding affinities than RAD-Lys-(Arg^{11})CCMSH. The differences in MC1 receptor binding affinities among these peptides were attributed to the subtle structural differences among the amino acids (Gly, Ala, Thr and Val). We further radiolabeled RTD-Lys-(Arg^{11})CCMSH and RVD-Lys-(Arg^{11})CCMSH with ^{99m}Tc and determined their biodistribution and tumor imaging properties in B16/F1

melanoma-bearing C57 mice. Both ^{99m}Tc-RTD-Lys-(Arg^{11})CCMSH and ^{99m}Tc-RVD-Lys-(Arg^{11})CCMSH were stable in mouse serum for 24 h at 37 °C. ^{99m}Tc-RTD-Lys-(Arg^{11})CCMSH and ^{99m}Tc-RVD-Lys-(Arg^{11})CCMSH showed similar patterns in cellular internalization and efflux in B16/F1 melanoma cells. ^{99m}Tc-RTD-Lys-(Arg^{11})CCMSH and ^{99m}Tc-RVD-Lys-(Arg^{11})CCMSH exhibited comparable high receptor-mediated melanoma uptake as ^{99m}Tc-RAD-Lys-(Arg^{11})CCMSH. However, the tumor uptake pattern was different between ^{99m}Tc-RTD-Lys-(Arg^{11})CCMSH and ^{99m}Tc-RVD-Lys-(Arg^{11})CCMSH. ^{99m}Tc-RTD-Lys-(Arg^{11})CCMSH showed the highest tumor uptake of 18.77 ± 5.13% ID/g at 2 h post-injection, whereas ^{99m}Tc-RVD-Lys-(Arg^{11})CCMSH reached the highest tumor uptake of 19.63 ± 4.68% ID/g at 4 h post-injection. Meanwhile, ^{99m}Tc-RVD-Lys-(Arg^{11})CCMSH exhibited lower renal uptake than ^{99m}Tc-RTD-Lys-(Arg^{11})CCMSH at 0.5, 2, and 4 h post-injection. The renal uptake of ^{99m}Tc-RVD-Lys-(Arg^{11})CCMSH was 62, 70, and 70% of the renal uptake of ^{99m}Tc-RTD-Lys-(Arg^{11})CCMSH at 0.5, 2, and 4 h post-injection, respectively.

The B16/F1 melanoma lesions could be clearly visualized by SPECT using ^{99m}Tc-RTD-Lys-(Arg^{11})CCMSH and ^{99m}Tc-RVD-Lys-(Arg^{11})CCMSH as imaging probes. Moreover, switching from the diagnostic ^{99m}Tc to therapeutic ^{188}Re/^{186}Re could further expand their therapeutic applications. Since ^{188}Re/^{186}Re share similar coordination chemistry with ^{99m}Tc, both RTD-Lys-(Arg^{11})CCMSH and RVD-Lys-(Arg^{11})CCMSH should be readily labeled with ^{188}Re/^{186}Re without structural modification of the peptides. Because the renal uptake of ^{99m}Tc-RVD-Lys-(Arg^{11})CCMSH was about 30% less than that of ^{99m}Tc-RTD-Lys-(Arg^{11})CCMSH, RVD-Lys-(Arg^{11})CCMSH could be a better candidate for melanoma therapy when labeled with ^{188}Re/^{186}Re. However, ^{99m}Tc-RVD-Lys-(Arg^{11})CCMSH displayed high non-specific renal uptake in this study. Thus, it is desirable to reduce the renal uptake to facilitate its therapeutic application. *L*-lysine co-injection dramatically decreased the renal uptake of ^{99m}Tc-RTD-Lys-(Arg^{11})CCMSH and ^{99m}Tc-RVD-Lys-(Arg^{11})CCMSH by 40–50% (Figure 5), suggesting that the overall positive charges of the ^{99m}Tc-RXD-Lys-(Arg^{11})CCMSH peptides played key roles in their non-specific renal uptake. The reduction of the overall positive charge of ^{111}In-DOTA-GlyGlu-CycMSH via a negatively-charged glutamic acid linker resulted in a decrease in renal uptake by 44% as compared to ^{111}In-DOTA-GlyGlu-CycMSH (11). Accordingly, it is likely that the reduction of the overall positive charges of the ^{99m}Tc-RXD-Lys-(Arg^{11})CCMSH peptides through the structural modification would decrease their non-specific renal uptake. It is worthwhile to note that four positively-charged amino acids, namely three arginines and one lysine linker, contributed to the overall positive charges of the ^{99m}Tc-RXD-Lys-(Arg^{11})CCMSH peptides. Because two arginines in the (Arg^{11})CCMSH motif are critical for MC1 receptor binding, the structural modification on the arginines in the (Arg^{11})CCMSH motif would likely decrease the receptor binding affinity of the peptide. Alternatively, the replacement of lysine linker or arginine in the RXD motif by neutral or negatively-charged amino acids would likely reduce the overall positive charges of ^{99m}Tc-RXD-Lys-(Arg^{11})CCMSH peptides without sacrificing their receptor binding affinities. It will be interesting to examine how the structural modification on the lysine linker or arginine in the RXD motif affects the tumor and renal uptake in future studies.

In conclusion, the substitution of Gly with Thr and Val retained low nanomolar MC1 receptor binding affinities of the peptides in B16/F1 melanoma cells. ^{99m}Tc-RVD-Lys-(Arg^{11})CCMSH exhibited comparable high melanoma uptake as ^{99m}Tc-RTD-Lys-(Arg^{11})CCMSH, but 30% less renal uptake than ^{99m}Tc-RTD-Lys-(Arg^{11})CCMSH. In spite of high receptor-mediated melanoma uptake, high non-specific renal uptake of ^{99m}Tc-RVD-Lys-(Arg^{11})CCMSH needs to be reduced to facilitate its future application.

Acknowledgments

We appreciate Dr. Fabio Gallazzi for his technical assistance. This work was supported in part by the NIH grant NM-INBRE P20RR016480/P20GM103451 and UNM RAC Award. The images were generated by the KUSAIR established with funding from the W.M. Keck Foundation and the UNM Cancer Research and Treatment Center (NIH P30 CA118100).

REFERENCES

1. Siegel R, Naishadham D, Jemal A. Cancer statistics. CA Cancer J. Clin. 2012; 62:10–29. [PubMed: 22237781]
2. Giblin MF, Wang N, Hoffman TJ, Jurisson SS, Quinn TP. Design and characterization of alpha-melanotropin peptide analogs cyclized through rhenium and technetium metal coordination. Proc. Natl. Acad. Sci. USA. 1998; 95:12814–12818. [PubMed: 9788997]
3. Froidevaux S, Calame-Christe M, Tanner H, Sumanovski L, Eberle AN. A novel DOTA-alpha-melanocyte-stimulating hormone analog for metastatic melanoma diagnosis. J. Nucl. Med. 2002; 43:1699–1706. [PubMed: 12468522]
4. Miao Y, Whitener D, Feng W, Owen NK, Chen J, Quinn TP. Evaluation of the human melanoma targeting properties of radiolabeled alpha-melanocyte stimulating hormone peptide analogues. Bioconjug. Chem. 2003; 14:1177–1184. [PubMed: 14624632]
5. Froidevaux S, Calame-Christe M, Schuhmacher J, Tanner H, Saffrich R, Henze M, Eberle AN. A Gallium-labeled DOTA-α-melanocyte-stimulating hormone analog for PET imaging of melanoma metastases. J. Nucl. Med. 2004; 45:116–123. [PubMed: 14734683]
6. McQuade P, Miao Y, Yoo J, Quinn TP, Welch MJ, Lewis JS. Imaging of melanoma using ^{64}Cu-and ^{86}Y-DOTA-ReCCMSH(Arg^{11}), a cyclized peptide analogue of alpha-MSH. J. Med. Chem. 2005; 48:2985–2992. [PubMed: 15828837]
7. Wei L, Butcher C, Miao Y, Gallazzi F, Quinn TP, Welch MJ, Lewis JS. Synthesis and biologic evaluation of ^{64}Cu-labeled rhenium-cyclized alpha-MSH peptide analog using a cross-bridged cyclam chelator. J. Nucl. Med. 2007; 48:64–72. [PubMed: 17204700]
8. Cheng Z, Xiong Z, Subbarayan M, Chen X, Gambhir SS. ^{64}Cu-labeled alpha-melanocyte-stimulating hormone analog for MicroPET imaging of melanocortin 1 receptor expression. Bioconjug. Chem. 2007; 18:765–772. [PubMed: 17348700]
9. Miao Y, Benwell K, Quinn TP. ^{99m}Tc-and ^{111}In-labeled alpha-melanocyte-stimulating hormone peptides as imaging probes for primary and pulmonary metastatic melanoma detection. J. Nucl. Med. 2007; 48:73–80. [PubMed: 17204701]
10. Miao Y, ; Figueroa SD, Fisher DR, Moore HA, Testa RF, Hoffman TJ, Quinn TP. ^{203}Pb-labeled alpha-melanocyte-stimulating hormone peptide as an imaging probe for melanoma detection. J. Nucl. Med. 2008; 49:823–829. [PubMed: 18413404]
11. Miao Y, Gallazzi F, Guo H, Quinn TP. ^{111}In-labeled lactam bridge-cyclized alpha-melanocyte stimulating hormone peptide analogues for melanoma imaging. Bioconjug. Chem. 2008; 19:539–547. [PubMed: 18197608]
12. Guo H, Shenoy N, Gershman BM, Yang J, Sklar LA, Miao Y. Metastatic melanoma imaging with an^{111}In-labeled lactam bridge-cyclized alpha-melanocyte-stimulating hormone peptide. Nucl. Med. Biol. 2009; 36:267–276. [PubMed: 19324272]
13. Guo H, Yang J, Gallazzi F, Miao Y. Reduction of the ring size of radiolabeled lactam bridge-cyclized alpha-MSH peptide resulting in enhanced melanoma uptake. J. Nucl. Med. 2010; 51:418–426. [PubMed: 20150256]
14. Guo H, Yang J, Gallazzi F, Miao Y. Effects of the amino acid linkers on melanoma-targeting and pharmacokinetic properties of Indium-111-labeled lactam bridge-cyclized α-MSH peptides. J. Nucl. Med. 2011; 52:608–616. [PubMed: 21421725]
15. Haubner R, Wester HJ, Reuning U, Senekowitsch-Schmidtke R, Diefenbach B, Kessler H, Stöcklin G, Schwaiger M. Radiolabeled alpha(v)beta(3) integrin antagonists: a new class of tracers for tumor targeting. J. Nucl. Med. 1999; 40:1061–1071. [PubMed: 10452325]

16. Poethko T, Schottelius M, Thumshirn G, Hersel U, Herz M, Henriksen G, Kessler H, Schwaiger M, Wester HJ. Two-step methodology for high-yield routine radiohalogenation of peptides: ^{18}F-labeled RGD and octreotide analogs. J. Nucl. Med. 2004; 45:892–902. [PubMed: 15136641]

17. Li C, Wang W, Wu Q, Ke S, Houston J, Sevick-Muraca E, Dong L, Chow D, Charnsangavej C, Gelovani JG. Dual optical and nuclear imaging in human melanoma xenografts using a single targeted imaging probe. Nucl. Med. Biol. 2006; 33:349–358. [PubMed: 16631083]

18. Decristoforo C, Faintuch-Linkowski B, Rey A, von Guggenberg E, Rupprich M, Hernandez-Gonzales I, Rodrigo T, Haubner R. [^{99m}Tc]HYNIC-RGD for imaging integrin alphavbeta3 expression. Nucl. Med. Biol. 2006; 33:945–952. [PubMed: 17127166]

19. Alves S, Correia JD, Gano L, Rold TL, Prasanphanich A, Haubner R, Rupprich M, Alverto R, Decristoforo C, Santos I, Smith CJ. In vitro and in vivo evaluation of a novel ^{99m}Tc(CO)$_3$-pyrazolyl conjugate of cyclo-(Arg-Gly-Asp-d-Tyr-Lys). Bioconjug. Chem. 2007; 18:530–537. [PubMed: 17373771]

20. Decristoforo C, Hernandez Gonzalez I, Carlsen J, Rupprich M, Huisman M, Virgolini I, Wester HJ, Haubner R. ^{68}Ga-and^{111}In-labelled DOTA-RGD peptides for imaging of alpha(v)beta(3) integrin expression. Eur. J. Nucl. Med. Mol. Imaging. 2008; 35:1507–1515. [PubMed: 18369617]

21. Hultsch C, Schottelius M, Auernheimer J, Alke A, Wester HJ. ^{18}F-Fluoroglucosylation of peptides, exemplified on cyclo(RGDfK). Eur. J. Nucl. Med. Mol. Imaging. 2009; 36:1469–1474. [PubMed: 19350236]

22. Wei L, Ye Y, Wadas TJ, Lewis JS, Welch MJ, Achilefu S, Anderson CJ. ^{64}Cu-labeled CB-TE2A and diamsar-conjugated RGD peptide analogs for targeting angiogenesis: comparison of their biological activity. Nucl. Med. Biol. 2009; 36:277–285. [PubMed: 19324273]

23. Yang J, Guo H, Miao Y. Technetium-99m-labeled Arg-Gly-Asp-conjugated alpha-melanocyte stimulating hormone hybrid peptides for human melanoma imaging. Nucl. Med. Biol. 2010; 37:873–883. [PubMed: 21055617]

24. Yang J, Miao Y. of Gly with Ala enhanced the melanoma uptake of technetium-99m-labeled Arg-Ala-Asp-conjugated alpha-melanocyte stimulating hormone peptide. Bioorg. Med. Chem. Lett. 2012; 22:1541–1545. [PubMed: 22297112]

25. Yang J, Guo H, Gallazzi F, Berwick M, Padilla RS, Miao Y. Evaluation of a novel RGD-conjugated alpha-melanocyte stimulating hormone hybrid peptide for potential melanoma therapy. Bioconjug. Chem. 2009; 20:1634–1642. [PubMed: 19552406]

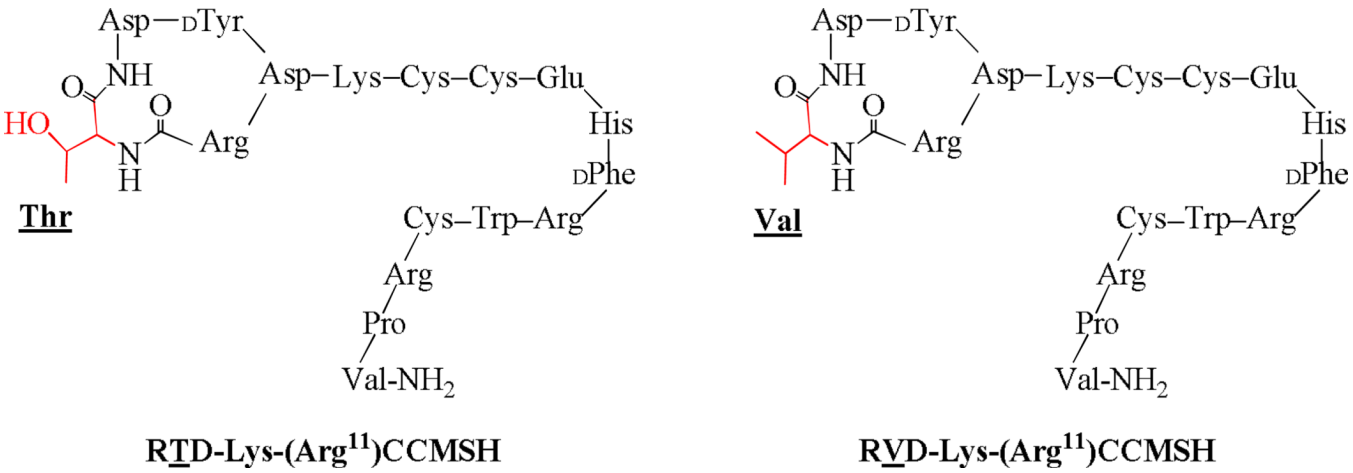

Figure 1.
Schematic structures of RTD-Lys-(Arg^{11})CCMSH and RVD-Lys-(Arg^{11})CCMSH.

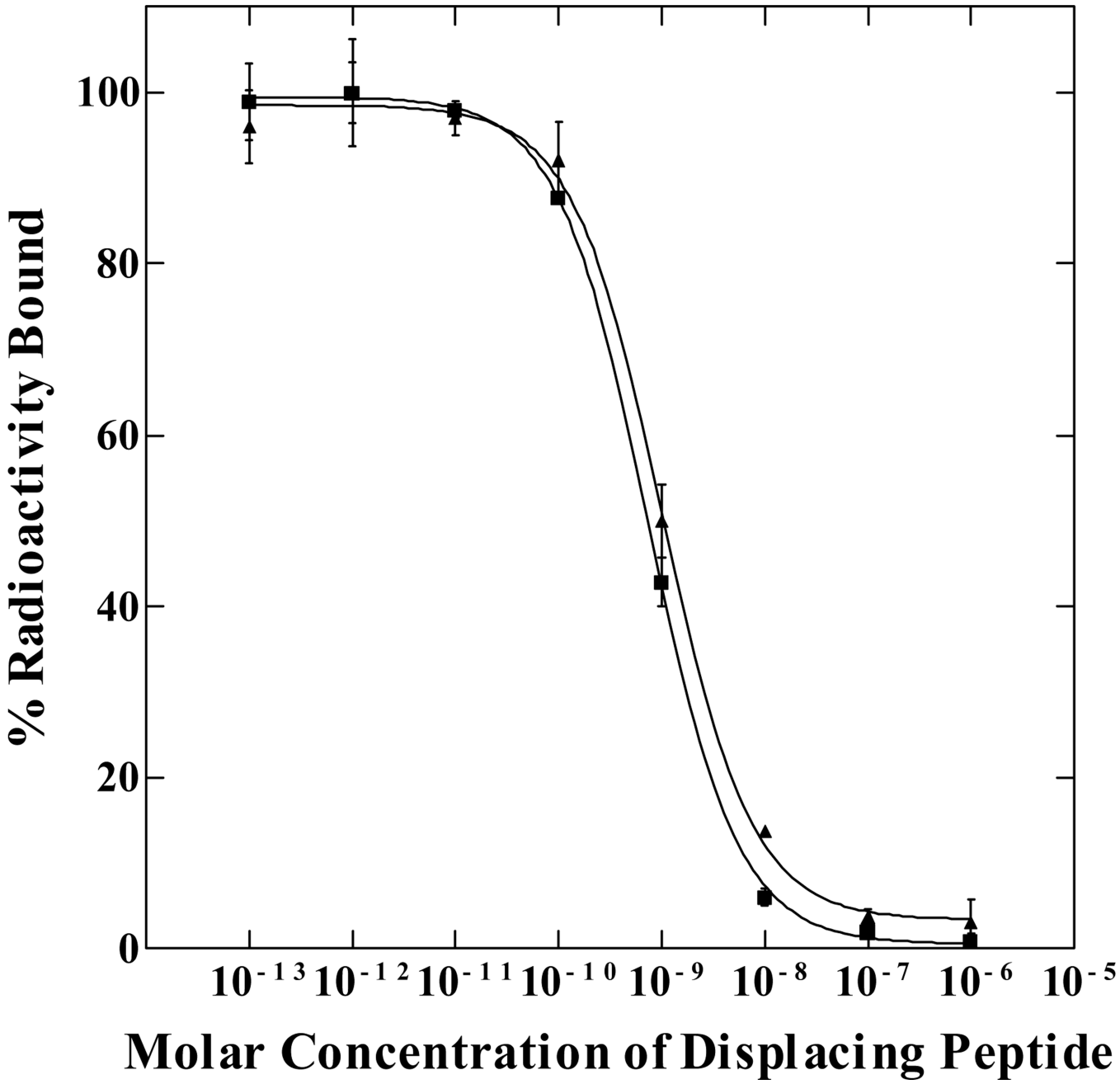

Figure 2.
The competitive binding curves of RTD-Lys-(Arg^{11})CCMSH (■) and RVD-Lys-(Arg^{11})CCMSH (▲) in B16/F1 melanoma cells. The IC_{50} value of RTD-Lys-(Arg^{11})CCMSH and RVD-Lys-(Arg^{11})CCMSH was 0.7 and 1.0 nM, respectively.

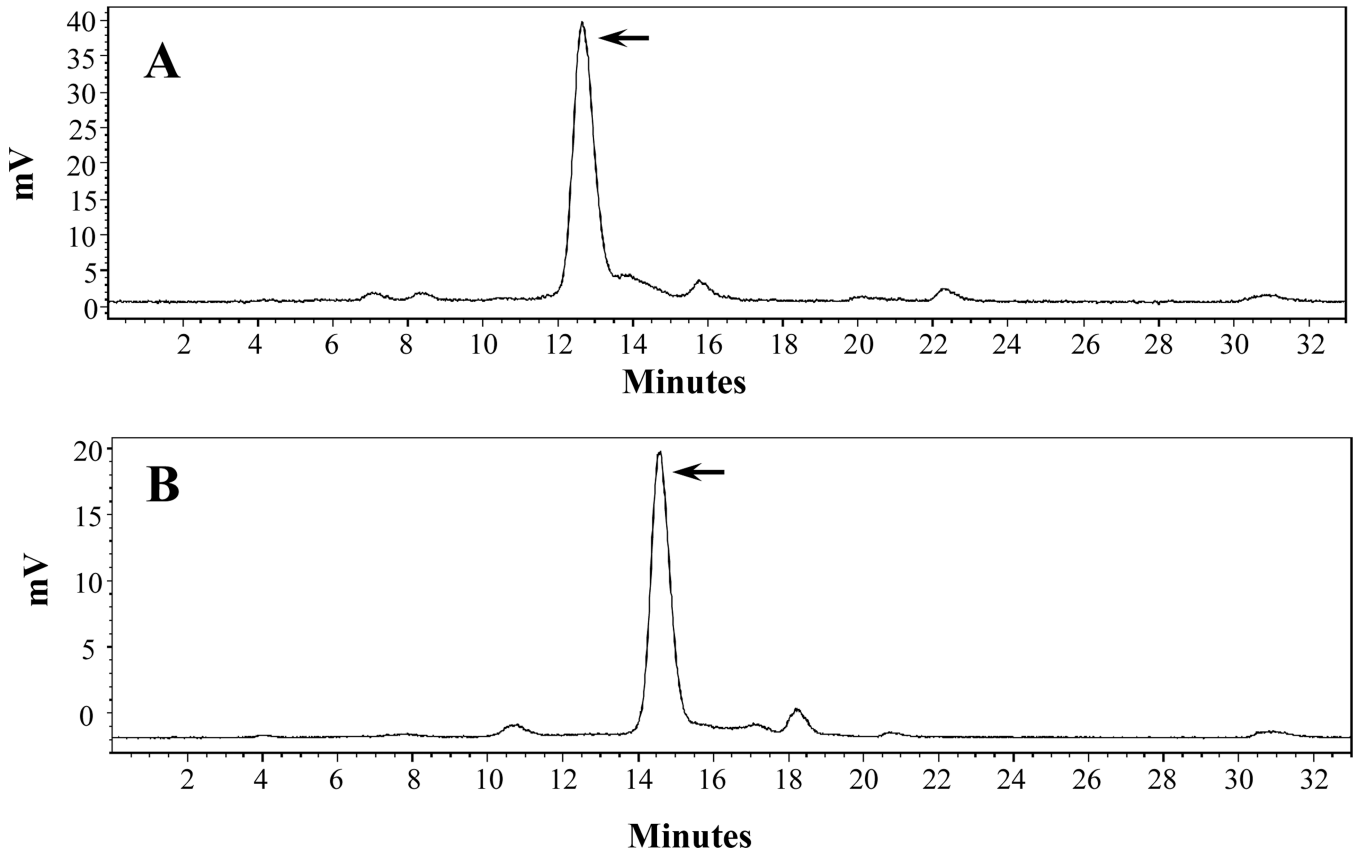

Figure 3.
Radioactive HPLC profiles of ^{99m}Tc-RTD-Lys-(Arg^{11})CCMSH (A) and ^{99m}Tc-RVD-Lys-(Arg^{11})CCMSH (B) in mouse serum after incubation at 37 °C for 24 h. The arrows denote the original retention times of ^{99m}Tc-RTD-Lys-(Arg^{11})CCMSH (12.7 min) and ^{99m}Tc-RVD-Lys-(Arg^{11})CCMSH (14.6 min) prior to the incubation in mouse serum.

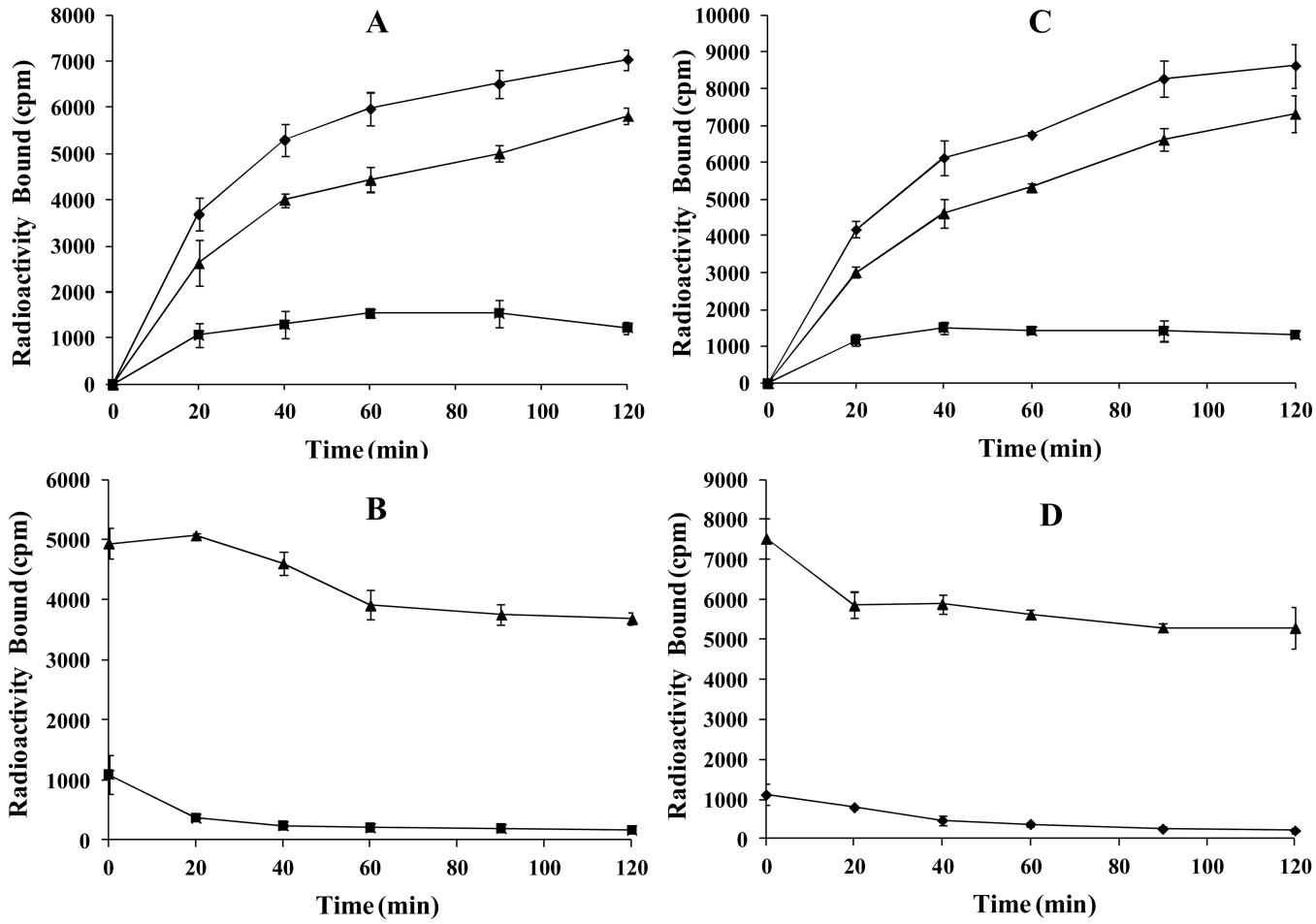

Figure 4.

Cellular internalization and efflux of ^{99m}Tc-RTD-Lys-(Arg^{11})CCMSH (A and B) and ^{99m}Tc-RVD-Lys-(Arg^{11})CCMSH (C and D) in B16/F1 melanoma cells. Total bound radioactivity (♦), internalized radioactivity (▲) and cell membrane radioactivity (■) were presented as counts per minute (cpm).

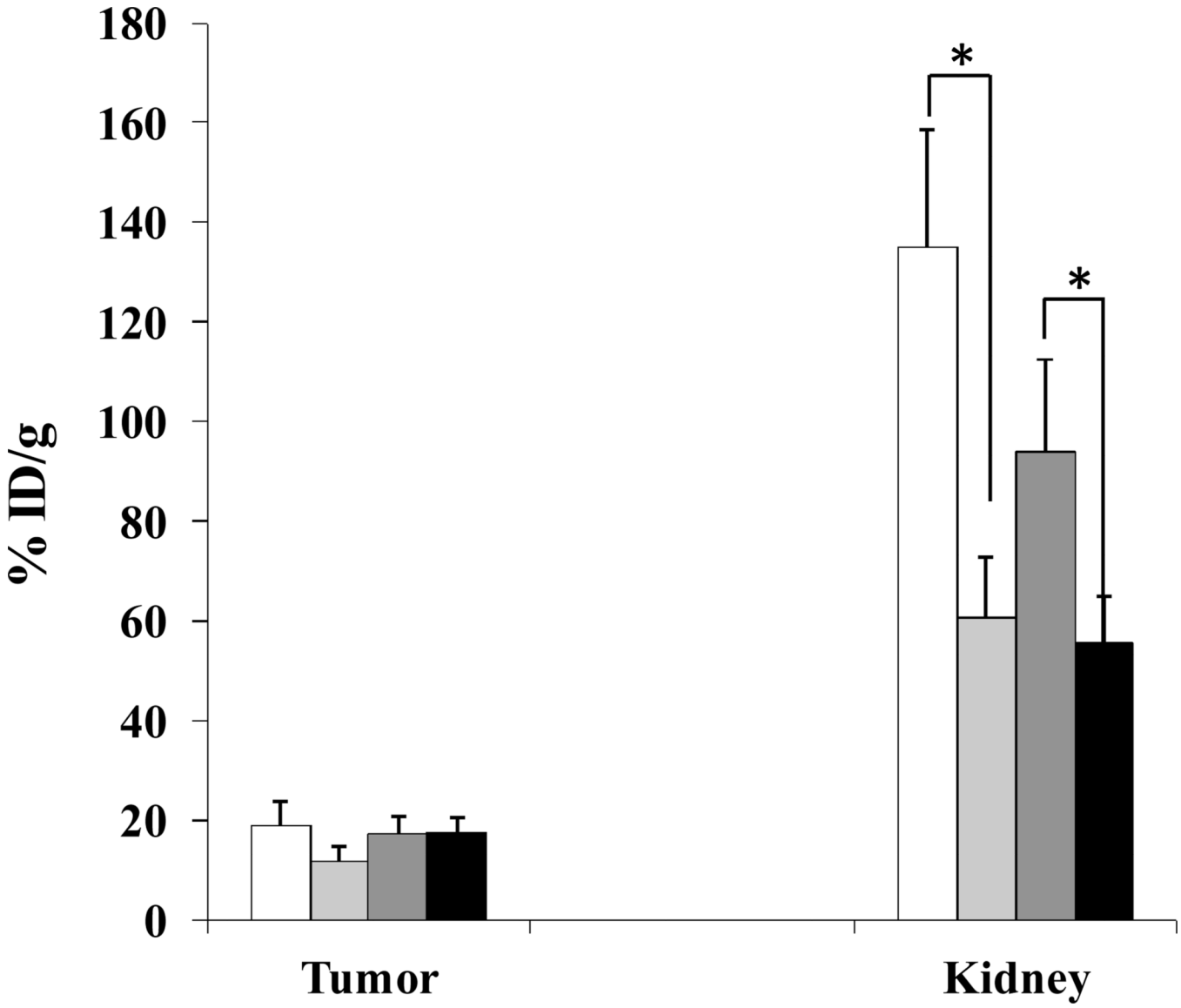

Figure 5.

Effect of *L*-lysine co-injection on the tumor and kidney uptakes of ^{99m}Tc-RTD-Lys-(Arg^{11})CCMSH and ^{99m}Tc-RVD-Lys-(Arg^{11})CCMSH at 2 h post-injection in B16/F1 melanoma-bearing C57 mice. The white (□) and light grey (▫) columns represented the tumor and renal uptake of ^{99m}Tc-RTD-Lys-(Arg^{11})CCMSH with or without *L*-lysine co-injection. The heavy grey (▪) and black (■) columns represented the tumor and renal uptake of ^{99m}Tc-RVD-Lys-(Arg^{11})CCMSH with or without *L*-lysine co-injection. *L*-lysine co-injection significantly (*$p<0.05$) reduced the renal uptake of ^{99m}Tc-RTD-Lys-(Arg^{11})CCMSH by 55% and the renal uptake of ^{99m}Tc-RVD-Lys-(Arg^{11})CCMSH by 41% at 2 h post-injection without affecting their tumor uptake.

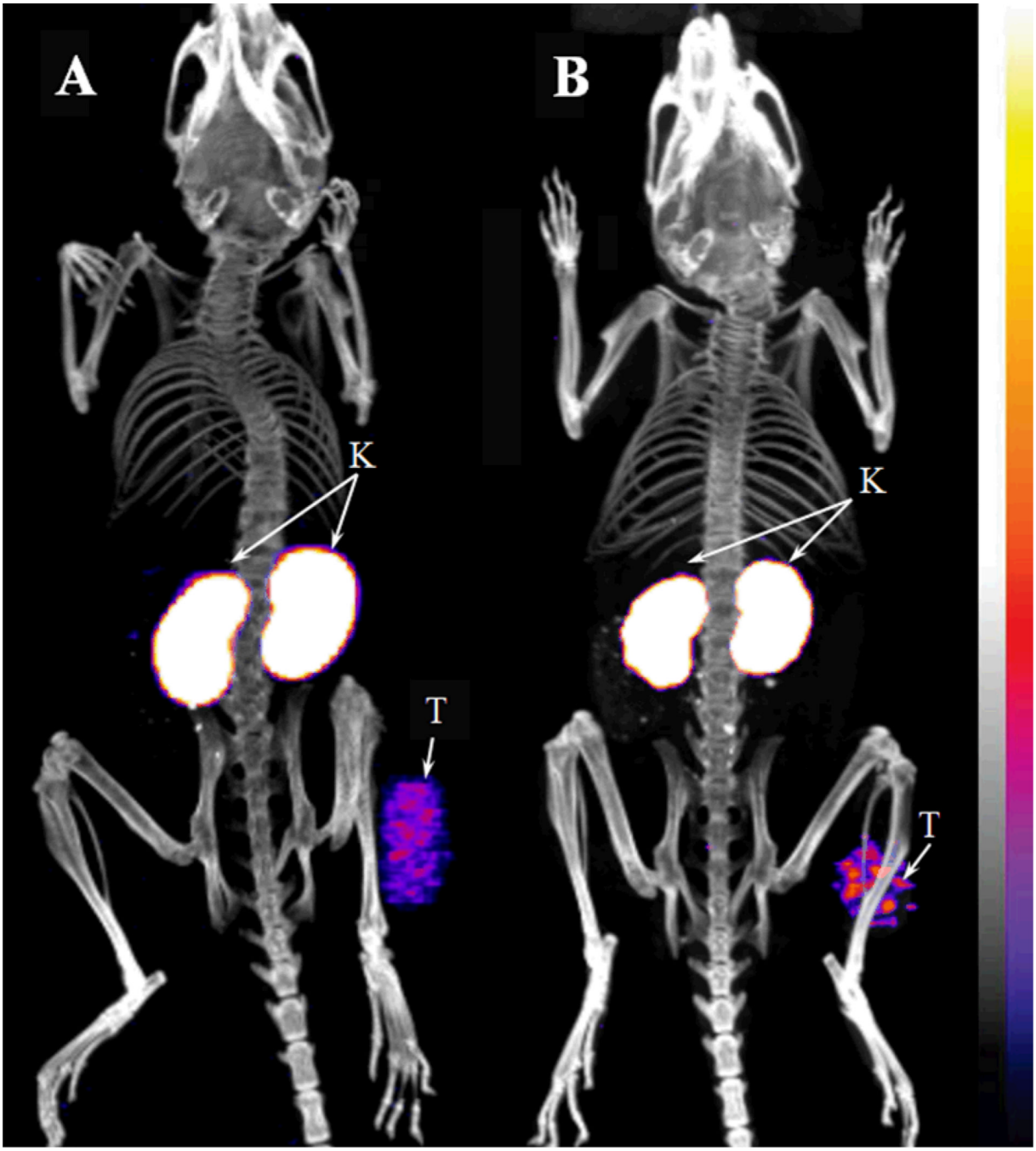

Figure 6.
Representative whole-body SPECT/CT images of B16/F1 melanoma-bearing C57 mice 2 h post injection of 7.4 MBq of ^{99m}Tc-RTD-Lys-(Arg^{11})CCMSH (A) and ^{99m}Tc-RVD-Lys-(Arg^{11})CCMSH (B). Flank melanoma lesions (T) and kidneys (K) were highlighted with arrows on the images.

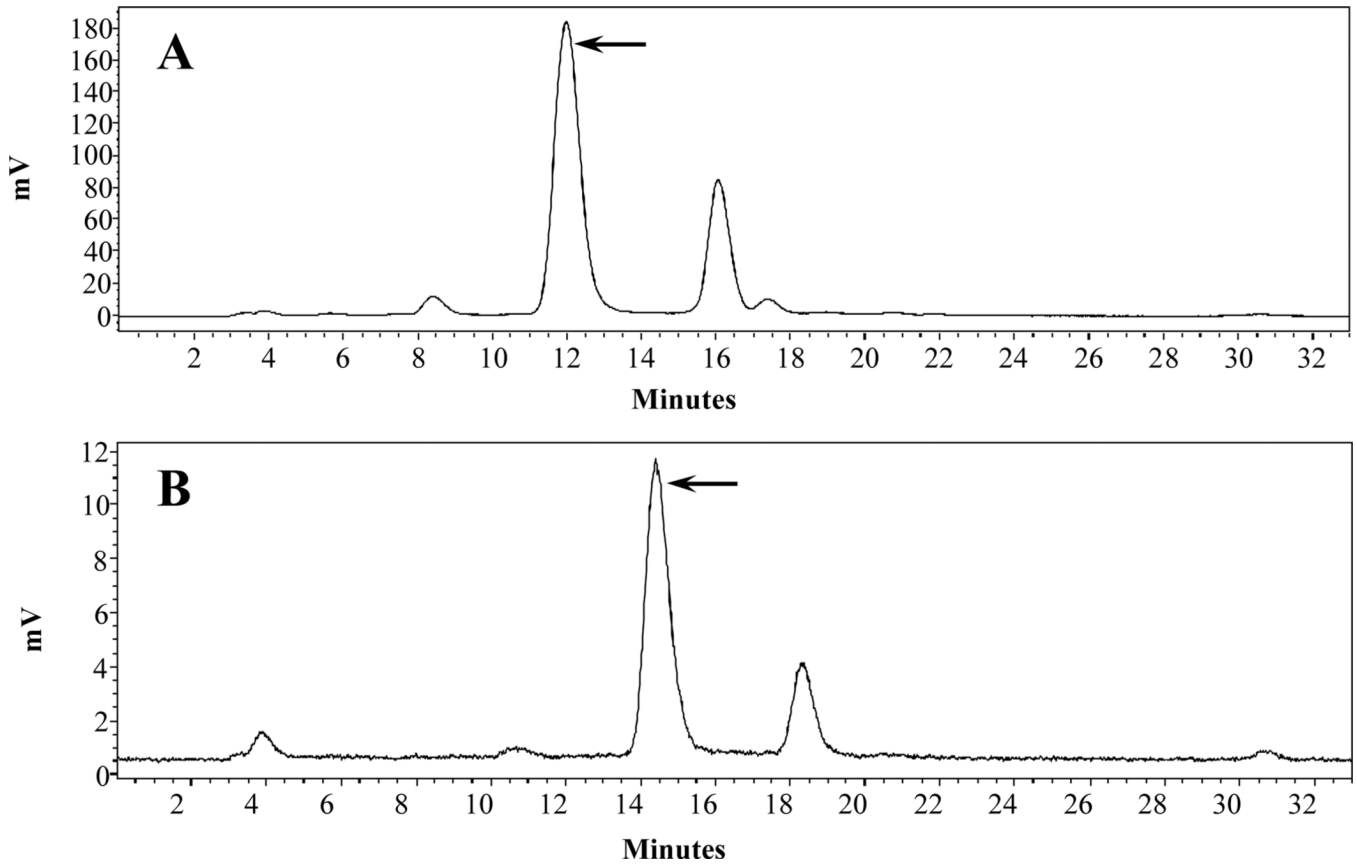

Figure 7.

Radioactive HPLC profiles of urinary metabolites at 2 h post-injection of ^{99m}Tc-RTD-Lys-(Arg^{11})CCMSH (A) and ^{99m}Tc-RVD-Lys-(Arg^{11})CCMSH (B). The arrows denote the original retention times of ^{99m}Tc-RTD-Lys-(Arg^{11})CCMSH (12.7 min) and ^{99m}Tc-RVD-Lys-(Arg^{11})CCMSH (14.6 min) prior to tail vein injection.

Mol Pharm. Author manuscript; available in PMC 2014 February 05.

Table 1

Biodistribution of ^{99m}Tc-RTD-Lys-(Arg^{11})CCMSH in B16/F1 melanoma-bearing C57 mice. The data was presented as percent injected dose/gram or as percent injected dose (mean ± SD, n=4).

Tissue	0.5 h	2 h	4 h	24 h	2 h NDP Blockade
			Percent injected dose/gram (%ID/g)		
Tumor	14.56 ± 5.31	18.77 ± 5.13	13.84 ± 3.10	5.84 ± 0.50	2.85 ± 1.43*
Brain	0.14 ± 0.04	0.03 ± 0.01	0.02 ± 0.01	0.03 ± 0.01	0.08 ± 0.06
Blood	15.95 ± 3.97	0.44 ± 0.13	0.55 ± 0.41	0.40 ± 0.21	0.50 ± 0.20
Heart	1.86 ± 0.21	0.29 ± 0.08	0.19 ± 0.05	0.12 ± 0.02	0.42 ± 0.26
Lung	4.27 ± 0.27	0.51 ± 0.37	0.39 ± 0.24	0.23 ± 0.04	1.18 ± 0.40
Liver	2.09 ± 0.04	1.62 ± 0.14	2.01 ± 0.39	1.03 ± 0.10	2.09 ± 0.64
Skin	3.99 ± 0.42	0.50 ± 0.19	0.27 ± 0.13	1.01 ± 0.31	1.21 ± 0.64
Spleen	1.04 ± 0.33	0.48 ± 0.20	0.47 ± 0.18	0.19 ± 0.13	0.64 ± 0.37
Stomach	1.87 ± 0.21	0.67 ± 0.16	0.70 ± 0.23	0.21 ± 0.04	1.11 ± 0.82
Kidneys	144.56 ± 24.64	135.14 ± 23.62	105.54 ± 27.67	46.84 ± 14.83	96.23 ± 28.13
Muscle	0.80 ± 0.38	0.15 ± 0.05	0.07 ± 0.02	0.52 ± 0.10	0.33 ± 0.03
Pancreas	0.83 ± 0.40	0.11 ± 0.04	0.09 ± 0.05	0.13 ± 0.07	0.44 ± 0.34
Bone	1.66 ± 0.10	0.46 ± 0.11	0.39 ± 0.12	0.23 ± 0.09	0.91 ± 0.59
			Percent injected dose (%ID)		
Intestines	1.73 ± 0.17	0.84 ± 0.20	0.72 ± 0.18	0.48 ± 0.13	1.16 ± 0.61
Urine	28.64 ± 8.85	54.76 ± 5.65	61.21 ± 5.56	82.19 ± 4.69	48.53 ± 21.62
			Uptake ratio of tumor/normal tissue		
Tumor/Blood	0.91	42.66	25.16	14.60	5.70
Tumor/Kidneys	0.10	0.14	0.13	0.12	0.03
Tumor/Lung	3.41	36.80	35.49	25.39	2.42
Tumor/Liver	6.97	11.59	6.89	5.67	1.36
Tumor/Muscle	18.20	125.13	197.71	11.23	8.64

*$p<0.05$ ($p=0.01$) for determining the significance of differences in tumor and kidney uptake between ^{99m}Tc-RTD-Lys-(Arg^{11})CCMSH with or without NDP-MSH peptide blockade at 2 h post-injection.

Mol Pharm. Author manuscript; available in PMC 2014 February 05.

Table 2

Biodistribution of ^{99m}Tc-RVD-Lys-(Arg^{11})CCMSH in B16/F1 melanoma-bearing C57 mice. The data was presented as percent injected dose/gram or as percent injected dose (mean ± SD, n=4).

Tissue	0.5 h	2 h	4 h	24 h	2 h NDP Blockade
Percent injected dose/gram (%ID/g)					
Tumor	16.70 ± 5.31	17.10 ± 3.82	19.63 ± 4.68	8.81 ± 2.13	1.51 ± 0.6*
Brain	0.15 ± 0.05	0.04 ± 0.01	0.02 ± 0.01	0.03 ± 0.01	0.03 ± 0.01
Blood	1.50 ± 0.52	0.49 ± 0.05	0.54 ± 0.45	0.07 ± 0.02	0.55 ± 0.35
Heart	0.74 ± 0.43	0.26 ± 0.15	0.16 ± 0.03	0.10 ± 0.07	0.26 ± 0.11
Lung	2.01 ± 0.97	0.87 ± 0.40	0.49 ± 0.43	0.19 ± 0.10	0.83 ± 0.24
Liver	1.86 ± 0.17	1.40 ± 0.34	1.59 ± 0.13	1.21 ± 0.26	1.32 ± 0.14
Skin	9.59 ± 0.62	0.69 ± 0.18	0.35 ± 0.08	0.42 ± 0.27	0.65 ± 0.10
Spleen	0.82 ± 0.43	0.40 ± 0.10	0.50 ± 0.15	0.34 ± 0.06	0.18 ± 0.14
Stomach	1.92 ± 0.53	1.21 ± 0.61	0.96 ± 0.27	0.40 ± 0.13	1.39 ± 0.79
Kidneys	90.19 ± 15.41	94.01 ± 18.31	73.92 ± 3.73	44.34 ± 12.11	67.24 ± 9.72
Muscle	11.25 ± 6.02	0.17 ± 0.10	0.10 ± 0.07	0.26 ± 0.02	0.03 ± 0.02
Pancreas	0.62 ± 0.25	0.10 ± 0.02	0.08 ± 0.08	0.18 ± 0.07	0.06 ± 0.03
Bone	1.6 ± 0.73	0.57 ± 0.08	0.54 ± 0.28	0.47 ± 0.05	0.46 ± 0.10
Percent injected dose (%ID)					
Intestines	1.36 ± 0.27	1.59 ± 1.08	0.95 ± 0.30	0.44 ± 0.22	1.36 ± 0.48
Urine	44.47 ± 3.12	59.2 ± 9.65	67.47 ± 10.00	76.85 ± 8.21	76.07 ± 3.55
Uptake ratio of tumor/normal tissue					
Tumor/Blood	11.13	34.89	36.35	125.86	2.75
Tumor/Kidneys	0.19	0.18	0.27	0.20	0.02
Tumor/Lung	8.31	19.66	40.06	46.37	1.82
Tumor/Liver	8.98	12.21	12.35	7.28	1.14
Tumor/Muscle	1.48	100.59	196.30	33.88	50.33

*$p<0.05$ ($p=0.002$) for determining the significance of differences in tumor and kidney uptake between ^{99m}Tc-RVD-Lys-(Arg^{11})CCMSH with or without NDP-MSH peptide blockade at 2 h post-injection.